Inhibition of triple-negative breast cancer proliferation and motility by reactivating p53 and inhibiting overactivated Akt

WEI CAO[1,2*], RENHUI SHEN[1*], SETH RICHARD[1], YU LIU[2], MOHAMMAD JALALIRAD[3], MARGOT P. CLEARY[1,4], ANTONIO B. D'ASSORO[3], SERGIO A. GRADILONE[1,4] and DA-QING YANG[1,4]

[1]The Hormel Institute, University of Minnesota, Austin, MN 55912, USA; [2]Sir Run Run Shaw Hospital, Nanjing Medical University, Nanjing, Jiangsu 211166, P.R. China; [3]Mayo Clinic, Rochester, MN 55905, USA; [4]The Masonic Cancer Center, University of Minnesota, Minneapolis, MN 55455, USA

Received March 20, 2021; Accepted October 25, 2021

DOI: 10.3892/or.2021.8252

Abstract. Mutations of p53 tumor suppressors occur more frequently in cancers at advanced stages or in more malignant cancer subtypes such as triple-negative breast cancer. Thus, restoration of p53 tumor suppressor function constitutes a valuable cancer therapeutic strategy. In the present study, it was revealed that a specific inhibitor of histone deacetylase 6, ACY-1215, caused increased acetylation of p53 in breast cancer cells with mutated p53, which was accompanied by increased expression of p21. These results suggested that ACY-1215 may lead to enhanced transcriptional activity of p53. It was also determined that ACY-1215 treatment resulted in G1 cell cycle arrest and apoptosis in these cancer cells. Furthermore, ACY-1215 displayed a synergistic effect with specific inhibitors of ATM, an activator of Akt, in inducing cancer cell apoptosis and inhibiting their motility. More importantly, it was observed that combination of ACY-1215 and ATM inhibitors exhibited markedly more potent antitumor activity than the individual compound in xenograft mouse models of breast cancer with mutant p53. Collectively, our results demonstrated that ACY-1215 is a novel chemotherapeutic agent that could restore mutant p53 function in cancer cells with strong antitumor activity, either alone or in combination with inhibitors of the ATM protein kinase.

Introduction

The p53 tumor suppressor plays critical roles in preventing malignant transformation. Under stressful conditions such as genotoxic stress, p53 is activated by multiple post-translational modifications including phosphorylation and acetylation (1,2). Activated p53 stimulates transcription of a variety of downstream genes leading to cell growth arrest, DNA repair, or apoptosis (1,2).

Triple negative breast cancer [TNBC; negative for estrogen receptor (ER), progesterone receptor, and HER2/neu] accounts for 15-20% of all breast cancers and is associated with the most aggressive clinical outcomes among different subtypes of breast cancer (3). Thus, there is an urgent need to find effective targeted therapeutic agents for treating advanced TNBC. Although TNBC only represents a fraction of all breast cancers, the majority of the p53 mutations in breast cancer occur in TNBC (3). These mutated p53 proteins affect different cellular functions, resulting in loss of cell cycle control, impairment of pro-apoptotic signaling pathways and defective cellular responses to DNA damage (4,5).

As p53 mutations are important in tumor aggressiveness and poor prognosis, restoring wild-type function of mutant p53 has been an intensive area of research (4,5). However, numerous of these attempts remain either in the early stage of development or have failed in clinical trials (2). It is thus essential to develop novel compounds that are capable of restoring function of p53 in cancers, including TNBC and other subtypes of breast cancer.

It is known that histone deacetylase 6 (HDAC6) inhibits p53 activity and p53-mediated cellular events through deacetylation of p53 (6). In addition, in breast cancers, HDAC6 overexpression is also correlated with increased mobility, migration and invasiveness of cancer cells (7). Therefore, it was hypothesized that inhibition of HDAC6 by its new inhibitors such as ACY-1215 (8) may restore p53 function in cancer cells.

In addition to mutated p53, the PI3K/Akt pathway is also dysregulated in the majority of TNBC, and it is known that these dysregulations cause over-activation of Akt, which leads to the development of cancer (9). Our previous studies have shown that a protein deficient in kinase ataxia telangiectasia's disease, ataxia-telangiectasia, mutated (ATM), is a stimulator of Akt (10,11). It was also revealed that a specific inhibitor of the ATM protein kinase, known as KU-55933, is capable of inhibiting Akt activity in TNBC and other types of breast cancer cells (9). In addition, our results indicated that KU-55933 suppressed proliferation of these breast cancer cells by inducing apoptosis (9).

Correspondence to: Dr Da-Qing Yang or Dr Sergio A. Gradilone, The Hormel Institute, University of Minnesota, 801 16th Avenue NE, Austin, MN 55912, USA
E-mail: dqyang2@hotmail.com; dyang@gundersenhealth.org
E-mail: sgradilo@umn.edu

*Contributed equally

Key words: ACY-1215, p53, KU-55933, KU-60019, ATM, triple-negative breast cancer

In the present brief study, the effect of ACY-1215 on p53-mediated cellular events in both MCF-7, a non-TNBC cell line (Luminal A and ER^+) with wild-type p53, and MDA-MB-231, a TNBC cell line with mutated p53 was first examined. Subsequently, a novel approach was examined to treat MDA-MB-231 and MCF-7 cells by combining ACY-1215 with KU-55933 or KU-60019, an analog of KU-55933. The results were also confirmed *in vivo* in a mouse model of TNBC. Our results validated ACY-1215, either as monotherapy or in combination with KU-55933 or KU-60019, as a promising new therapeutic agent for TNBC.

Materials and methods

Chemicals and reagents. Antibodies against poly ADP-ribose polymerase (PARP), p21, acetylated p53 at Lys-382 were obtained from Cell Signaling Technology, Inc. The anti-β-actin antibody was purchased from Sigma-Aldrich; Merck KGaA. KU-55933 and KU-60019 were purchased from Merck KGaA. ACY-1215 was purchased from APeXBIO Technology LLC.

Cell culture and protein assessment. MDA-MB-231 (HTB-26) and MCF-7 (HTB-22) cells were purchased from American Type Culture Collection (ATCC) and were cultured at 37˚C in either RPMI-1640 medium (product no. 10-040-CV) or DMEM (product no. 10-013-CV; both from Corning, Inc.) medium supplemented with antibiotics (penicillin and streptomycin; 1:100 dilution; Gibco; Thermo Fisher Scientific, Inc.) and 10% fetal bovine serum (FBS; cat. no. 26140-079; Gibco; Thermo Fisher Scientific, Inc.), respectively. Cells were lysed with TGN lysis buffer containing protease inhibitor cocktails (Roche Diagnostics). The protein concentration was determined by the BCA method.

Immunoblotting detection of proteins. Equal amounts of protein (50-80 μg) were subjected to SDS-PAGE (4-12%) and then transferred to a PVDF membrane. After blocking (5% milk in TBST for 2 h at RT), PVDF membranes were incubated with the following primary antibodies: Acetyl-p53 (Lys382) (1:1,000; product no. 2525), p21 Waf1/Cip1 (1:1,000; product no. 2947), PARP (46D11) (1:1,000; product no. 9532), acetyl-α-tubulin (K40) (D2063) (1:1,000; product no. 5335; all from Cell Signaling Technology, Inc), β-actin (1:2,000; product no. A2228), acetyl-p53 (Lys320) (1:200; product no. 06-1283; both from Sigma-Aldrich; Merck KGaA), HDAC6 (D-11) (1:100; cat. no. sc-28386) and p53 (DO-1) (1:500; cat. no. sc-126; both from Santa Cruz Biotechnology, Inc.) at 4˚C overnight, and HRP-conjugated secondary antibody (1:3,000; product code ab97051 or product code ab97023; Abcam) for 45 min at room temperature. The images were developed using SuperSignal™ West Pico PLUS chemiluminescent substrate (cat. no. 34580; Thermo Fisher Scientific, Inc.) following the manufacturer's protocol and visualized using Amersham Imager 600. Densitometric analysis was performed with the Amersham Imager 600 Analysis Software, V 1.0.0, from GE/General Electric.

Flow cytometric assay. Cells were cultured to sub-confluence and then treated (37˚C) with 10 μM ACY-1215 for 24 h. Cells were then harvested and fixed overnight at -20˚C with cold 70% ethanol. Cells ($1x10^6$/ml) were then treated with RNase and stained with propidium iodide at room temperature in the dark for 30 min (Sigma Aldrich; Merck KGaA). Cell cycle distribution at the G1 and S phases was analyzed by flow cytometry (FACSCalibur; and CellQuest software version 6.0f9; both from BD Biosciences), and cell cycle arrest was presented as G1/S ratios as previously described (9).

MTT cell viability assay. Cells ($1x10^6$/ml) were seeded in 48- or 96-well plates and cultured (37˚C) to sub-confluence. Following serum starvation for 24 h, the cells were then treated with ACY-1215, KU-55933 and/or KU-60019 (10 μM each) for 72 h at 37˚C. The ratio of viable cells in each well was determined using a CellTiter Nonradioactive Cell Proliferation Assay kit (cat. no. G400; Promega Corporation) according to the manufacturer's protocol. The Solubilization Solution/Stop Mix (included in the kit) was then added to the culture wells to solubilize the formazan product, and the absorbance at 570 nm was recorded using a plate reader.

IncuCyte cell proliferation assay. Cells were seeded at 40,000/well in 48-well plates in cell culture medium containing 2% FBS. Following the addition of chemical compounds (ACY-1215, KU-55933 and/or KU-60019; 10 μM each), the plates were placed in the IncuCyte S3 Live-Cell Analysis System (Essen BioScience) where real-time images were captured every 6 h for 72-96 h at a magnification of x10 for the entire experiment. The confluence of each group of cells was evaluated and plotted with the IncuCyte S3 2019A software (Essen BioScience).

Cell migration assay. MDA-MB-231 cells ($1x10^6$/ml) were seeded in a 6-well plate and were allowed to proliferate. Following the formation of a confluent monolayer (near 100%), the cells were scratched with a 200-μl sterile tip. Cells (which were serum-starved) were then washed with PBS and treated with different chemical compounds (10 μM ACY-1215 ± KU-55933 or KU-60019; KU55 alone; KU60 alone; as well as a control/vehicle (DMSO): Con; ACY, KU55, KU60, ACY + KU55, ACY + KU60). Images of the extent of cell migration (0 and 24 h) were captured with an inverted light microscope.

Cell invasion assay. Cells ($1x10^6$/ml) suspended in serum-free medium were seeded into the upper well of the invasion chamber (pore size 8 μm; cat. no. 08-774-122; Corning, Inc.). Medium containing 10% FBS was added to the bottom well of the chamber to serve as a chemoattractant. Chemical reagents (Con, ACY-1215, KU55 + ACY-1215, KU60 + ACY-1215) were added to both the upper and bottom layer of the chamber. Following incubation at 37˚C for 24 h, the cells on the upper surface of the filters were wiped away with a cotton swab. The filters were fixed with 2% paraformaldehyde followed by staining with 0.1% crystal violet for 10 min each at room temperature. The number of invasive cells were quantified under a light microscope.

Animal study. A total of 30 female athymic nude-*Foxn1*^{nu} mice (10-12 weeks old; Envigo) were injected at the left and/or right flank with $1x10^6$ MDA-MB-231 cells in PBS-Matrigel (BD Biosciences). The housing conditions were as follows: 68-74˚F; 30-70% humidity; and 12-h light/dark cycle, with full access to food and water. Experiments were performed in the date range of 3/12/2020 to 7/10/2020. After the tumors became

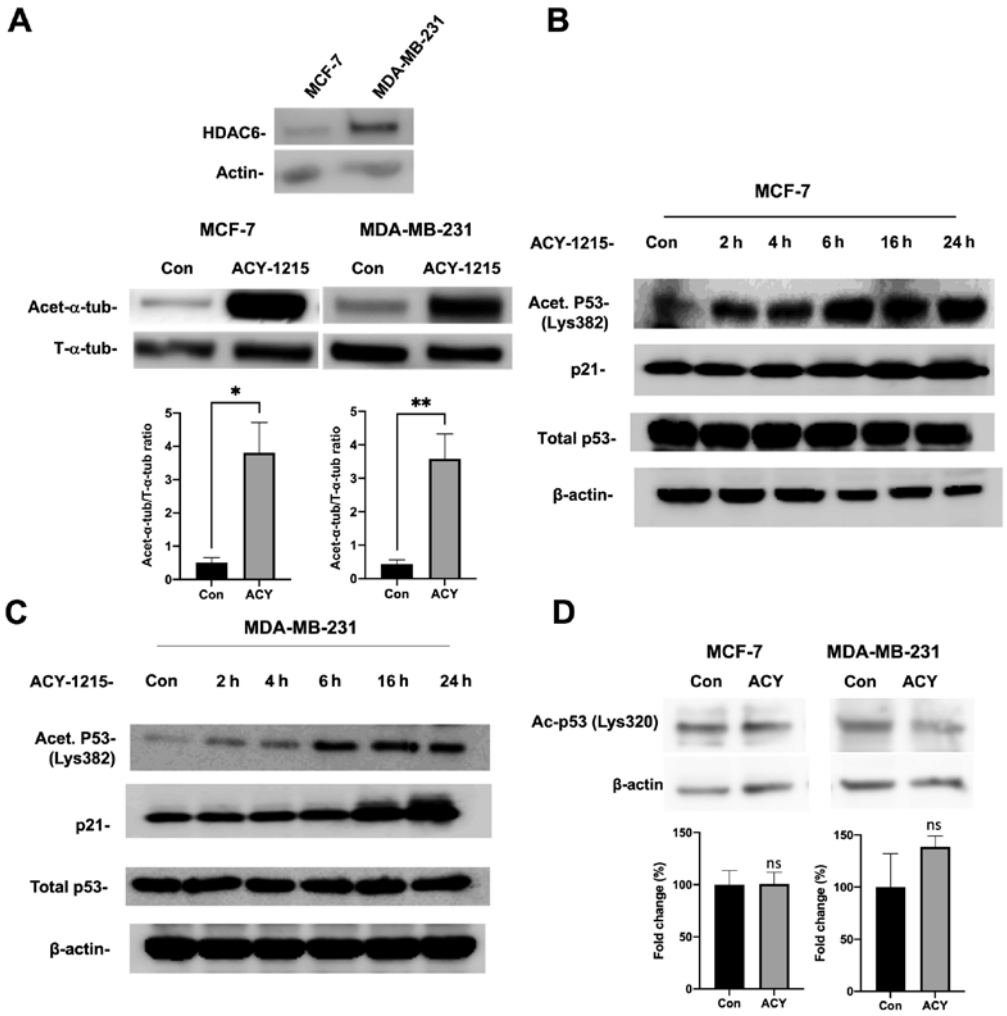

Figure 1. Inhibition of HDAC6 by ACY-1215 leads to increased p53 acetylation at Lys382, and enhanced expression of p21. (A) HDAC6 expression levels in MCF-7 and MDA-MB-231 cells were confirmed by western blotting (upper panel). Furthermore, cells were cultured to sub-confluence and then treated with 10 μM ACY-1215 for 24 h, and the levels of acetylated α-tubulin (Acet-α-tub) were assessed by immunoblotting (lower panel). (B and C) MCF-7 (B) and MDA-MB-231 (C) cells were cultured to sub-confluence and then treated with 10 μM ACY-1215 for the indicated time-points. p53 acetylation at Lys382, total p21, total p53, and β-actin were detected by immunoblotting. The results in B and C are representative of three individual experiments. (D) MCF-7 and MDA-MB-231 cells were cultured to sub-confluence and then treated with 10 μM ACY-1215 for 24 h. Levels of p53 acetylation at Lys320 were assessed by immunoblotting. *P<0.05 and **P<0.01. HDAC6, histone deacetylase 6.

visible (~40-50 mm^3), the mice with roughly equal tumor burden were divided into four groups. One group was intraperitoneally injected with vehicle and the other groups were injected with 30 mg/kg ACY-1215 (8), 1 mg/kg KU-55933 (12), or the combination. Tumor volumes were calculated according to the following formula: Volume = (width)^2 x length/2. Width and length of the tumors were measured using an electronic digital caliper with a resolution of 0.01 mm. Tumor volumes and body weight were recorded weekly and tumor weight and sizes were measured with the diameter of the largest tumor at 12 mm. Following four weeks of treatment, the mice were euthanized via a primary method of carbon dioxide euthanasia (flow rate of carbon dioxide used was ~30% chamber volume displaced/min), followed by a secondary method of cervical dislocation. Tumor samples were then removed. All the procedures were approved (IACUC Protocol 1905-37107A) by the University of Minnesota IACUC committee (Minneapolis, MN, USA).

Statistical analysis. Comparisons between two groups were evaluated by a Student's paired t-test and one-way ANOVA followed by Tukey's post hoc test was used to compare means of multiple groups with GraphPad Prism v. 9 (GraphPad Software, Inc.). Data are presented as the mean ± standard error and P<0.05 was considered to indicate a statistically significant difference.

Results

ACY-1215 causes increased p53 acetylation and induces p21 in breast cancer cells. As aforementioned, HDAC6 inhibits p53 activity and p53-mediated cellular events through deacetylation of p53 at Lys382 (6), and ACY-1215 is a newly developed specific HDAC6-inhibitor (8). Therefore, the effect of ACY-1215 was first examined on p53 acetylation and induction of p21, a downstream target of p53, in MCF-7 and MDA-MB-231 cells. First, HDAC6 expression in these cell lines was confirmed and ACY-1215 efficacy in the inhibition of HDAC6 was assessed by western blotting. The well-established substrate, α-tubulin, was identified as an indirect read out of ACY-1215 inhibiting HDAC6 activity, and therefore increased acetylated-α-tubulin levels (Fig. 1A). Then, our

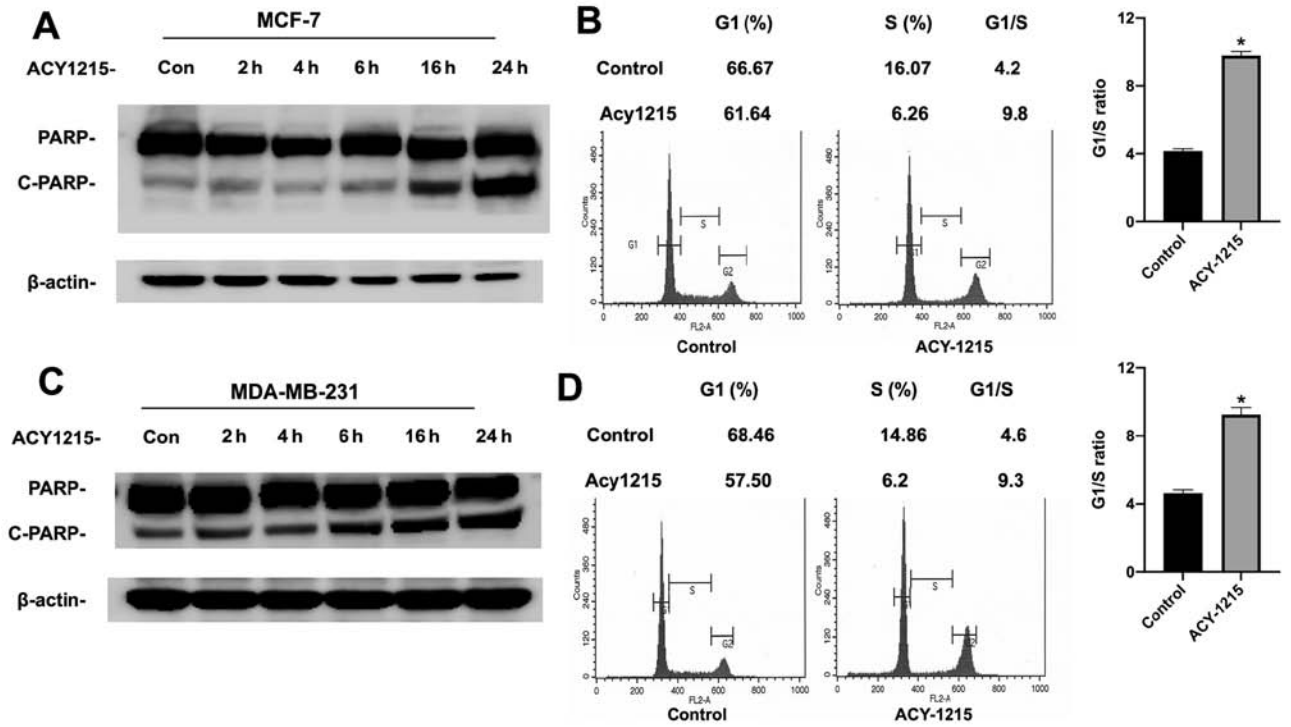

Figure 2. Inhibition of histone deacetylase 6 by ACY-1215 leads to increased apoptosis and G1 cell cycle arrest. (A and C) MCF-7 (A) and MDA-MB-231 (C) cells were cultured to sub-confluence and then treated with 10 μM ACY-1215 for the indicated time-points. Both floating and attached cells were collected following treatment. Cells were then lysed with TGN lysis buffer. Equal amounts of protein were subjected to SDS-PAGE and later transferred onto PVDF membranes. PARP/cleaved PARP and β-actin were detected by immunoblotting. (B and D) MCF-7 (B) and MDA-MB-231 (D) cells were cultured to sub-confluence and then treated with 10 μM ACY-1215 for 24 h. Cells were then harvested and fixed with ethanol. Cell cycle distribution at the G1 and S phases was analyzed by flow cytometry following propidium iodide staining of the cells as described in Materials and methods. Cell cycle arrest was presented as the G1/S ratio ± SEM from 3-4 replicates. *P<0.05.

results showed that ACY-1215 caused increased acetylation of p53 in MCF-7 cells (Fig. 1B). Additionally, this increased acetylation was accompanied by increased expression of p21, suggesting that ACY-1215 may lead to enhanced transcriptional activity of p53. Next, MDA-MB-231 cells were treated with ACY-1215 and it was determined that this inhibitor also caused increased acetylation of p53 (Fig. 1C). To our surprise, our results showed that this increased acetylation was also accompanied by increased expression of p21, suggesting that the inhibition of HDAC6 may lead to enhanced transcriptional activity of p53 in MDA-MB-231 cells as well. Furthermore, the effects of ACY-1215 appear to mainly target p53 Lys382, as no significant differences were observed at Lys320 (Fig. 1D).

ACY-1215 induces apoptosis and G1 cell cycle arrest in breast cancer cells. Since p53 controls cellular function by both inducing cell cycle arrest at the G1 phase and apoptosis in cancer cell lines, the effect of ACY-1215 on these p53-mediated cellular events was next examined in both MCF-7 and MDA-MB-231 cells. It was determined that ACY-1215 treatment resulted in both apoptosis, revealed by increased cleavage of PARP (Fig. 2A), a substrate of caspase-3, and G1 cell cycle arrest in MCF-7 cells (Fig. 2B). More importantly, it was also observed that ACY-1215 treatment led to increased apoptosis (Fig. 2C) and G1 cell cycle arrest (Fig. 2D) in MDA-MB-231 cells.

Combination of ACY-1215 and KU-55933 or KU-60019 induces markedly stronger apoptosis and is more effective in inhibiting MDA-MB-231 cell proliferation. Since the majority of the TNBC cells contain both p53 mutations and over-activated Akt, and the specific ATM inhibitors KU-55933 and KU-60019 inhibit Akt activity (13), a novel approach was next examined to target TNBC cells by combining ACY-1215 with KU-55933 or KU-60019. It was revealed that while ACY-1215 or KU-55933/KU-60019 as single agent could cause increased cellular apoptosis, combination of ACY-1215 with KU-55933 or KU-60019 led to markedly stronger apoptosis in MDA-MB-231 cells (Fig. 3A), suggesting an additive or synergistic effect of ACY-1215 and KU-55933 or KU-60019 on inducing apoptosis in MDA-MB-231 cells.

Next, the combination effect of ACY-1215 with KU-55933 or KU-60019 on MDA-MB-231 cells proliferation was determined. First, the effect of ACY-1215 ± KU-55933/KU-60019 on MDA-MB-231 cells proliferation was examined using MTT assays and a stronger effect was identified (Fig. 3B). To further examine the effect of these inhibitors, their effects were tested using the IncuCyte S3 Live-Cell Analysis System. Following treatment of MDA-MB-231 cells with ACY-1215 and KU-55933 or KU-60019, the inhibitory effects of either ACY-1215 or KU-55933 or KU-60019 on proliferation of MDA-MB-231 cells were again observed, yet the combination of these drugs revealed a significantly stronger suppressive effect on the proliferation of MDA-MB-231 cells (Fig. 3C).

Combination of ACY-1215 with KU-55933 or KU-60019 induces markedly stronger apoptosis and inhibits MCF-7 cell proliferation. Next, it was examined whether combination of

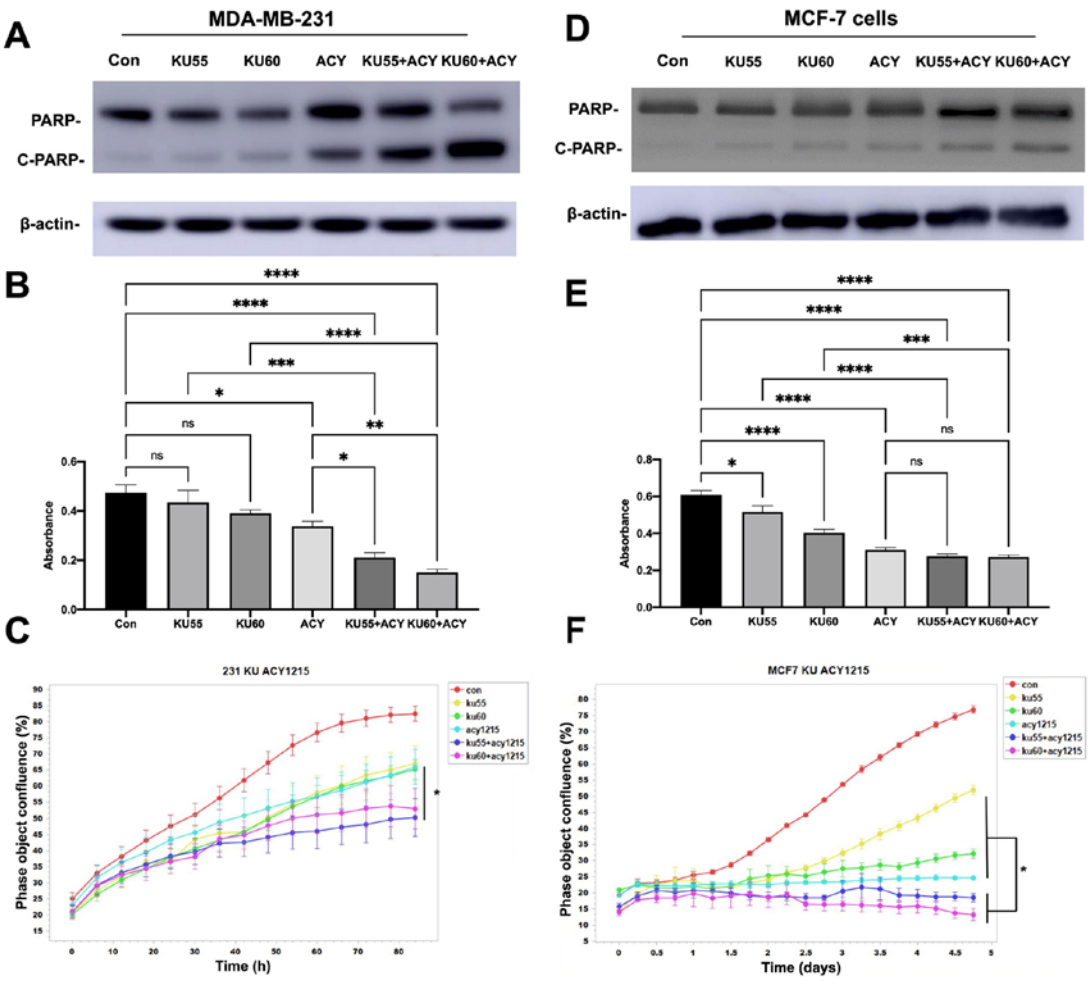

Figure 3. Combination of ACY-1215 with KU-55933 or KU-60019 has a stronger inhibitory effect on survival and proliferation than treatment with individual compounds alone. (A) MDA-MB-231 cells were serum-starved overnight and then treated with ACY-1215, KU-55933, and/or KU-60019 (10 μM each) for 24 h. Both floating and attached cells were collected following treatment. Cells were lysed by TGN lysis buffer, and cell lysates were subjected to SDS-PAGE. PARP, cleaved PARP, and β-actin were detected. The results are representative of three individual experiments. (B) MDA-MB-231 cells were plated on a 48-well plate and cultured to sub-confluence. Following serum starvation for 24 h, MDA-MB-231 cells were then treated with ACY-1215, KU-55933 and/or KU-60019 (10 μM each) for 72 h and MTT assays were performed. Results are presented as the absorbance ± SEM (C) MDA-MB-231 cells were plated on a 48-well plate and cultured in the presence of 2% FBS and in the absence or presence of ACY-1215, KU-55933 and/or KU-60019 (10 μM each) for 120 h, and the cell proliferation was determined by IncuCyte real-time imaging. Data are expressed as the change in percent confluence from 3-5 repeats. Treatments are labeled as control (red), KU-55933 (yellow), KU-60019 (green), ACY-1215 (light blue), KU-55933 + ACY-1215 (blue), and KU-60019 + ACY-1215 (purple). (D) MCF-7 cells were serum-starved overnight and then treated with ACY-1215, KU-55933, and/or KU-60019 (10 μM each) for 24 h. Both floating and attached cells were collected following treatment. Cells were lysed by TGN lysis buffer, and cell lysates were subjected to SDS-PAGE. PARP, cleaved PARP, and β-actin were detected. The results are representative of three individual experiments. (E) MCF-7 cells were plated on a 48-well plate and cultured to sub-confluence. Following serum starvation for 24 h, MCF-7 cells were then treated with ACY-1215, KU-55933 and/or KU-60019 (10 μM each) for 72 h, and an MTT assay was then performed. Results are presented as the absorbance ± SEM. (F) MCF-7 cells were plated on a 48-well plate and cultured in the presence of 2% FBS and in the absence or presence of ACY-1215, KU-55933 and/or KU-60019 (10 μM each) for 120 h, and the cell proliferation was evaluated by IncuCyte real-time imaging. Data are expressed as the change in percent confluence from 3-5 repeats. Treatments are labeled as control (red), KU-55933 (yellow), KU-60019 (green), ACY-1215 (light blue), KU-55933 + ACY-1215 (blue), and KU-60019+ACY-1215 (purple). *P<0.05, **P<0.01, ***P<0.001 and ****P<0.0001.

ACY-1215 with KU-55933 or KU-60019 could also induce stronger apoptosis in MCF-7 cells as MCF-7 also display high Akt activity (9). Similarly, while our results showed that ACY-1215 or KU-55933/KU-60019 alone could lead to increased apoptosis or cleavage of PARP, the combination of ACY-1215 with either KU-55933 or KU-60019 had a markedly stronger effect on inducing apoptosis in MCF-7 cells (Fig. 3D).

Next, the effect of combination of ACY-1215 with KU-55933 or KU-60019 on proliferation of MCF-7 cells was also evaluated using both MTT assay and the IncuCyte S3 Live-Cell Analysis System. Results from both assays demonstrated that whereas individual compound including ACY-1215 or KU-55933/KU-60019 could inhibit MCF-7 cell proliferation, combination of ACY-1215 with KU-55933 or KU-60019 also had a more potent effect on inhibiting cell proliferation of MCF-7 cells (Fig. 3E and F).

Noteworthy, the proliferation assays indicated that MCF-7 cells were slightly more sensitive to the double treatment compared with MDA-MB-231 cells. Conversely, PARP cleavage was more prominent in MDA-MB-231 cells than MCF-7 cells. Perhaps, the different levels of HDAC6 expression (Fig. 1A) may explain the distinct response of cell proliferation between the two cell lines rendering MCF-7 more sensitive to ACY-1215 than MDA-MB-231. To keep the results consistent,

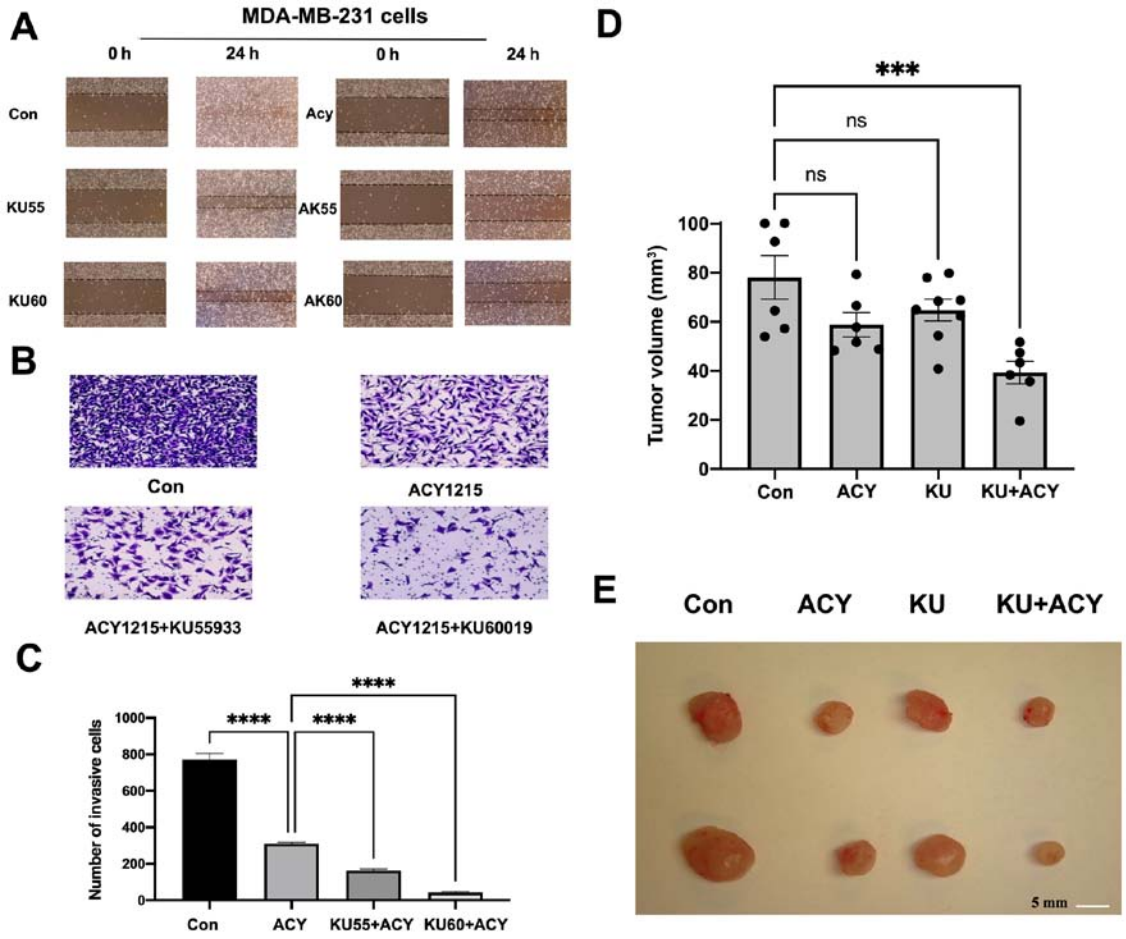

Figure 4. Combination of ACY-1215 with KU-55933 or KU-60019 has a stronger inhibitory effect on migration and invasion, and markedly reduces tumor growth *in vivo* compared with treatment with individual compounds alone. (A) MDA-MB-231 cells were seeded in a 6-well plate. Following forming a confluent monolayer, the cells were scratched with a 200-μl sterile tip. Cells were then treated with ACY-1215 ± KU-55933 or KU-60019 (10 μM each) as indicated for 24 h. Images of the cell migration were captured with an inverted microscope (magnification, x20). The results are representative of three experiments. (B and C) MDA-MB-231 cells suspended in serum-free medium were seeded into the upper well of the invasion chamber. Medium containing 10% FBS was added to the bottom well of the chamber to serve as a chemoattractant. ACY-1215 ± KU-55933 or KU-60019 (10 μM each) were added to both wells of the chamber. Following 24 h of incubation, the cells on the upper surface of the filters were wiped away. (B) The filters were stained with crystal violet and images were captured (magnification, x100). (C) Number of invasive cells on the filter were quantified under a microscope, and the number of cells ± SEM from 3 replicates are presented. (D) Female nude-*Foxn1*^{nu} mice were injected with 1x10^6 MDA-MB-231 cells into the left and/or right flanks as described in the Materials and methods. After the tumors became visible, the mice were divided into four groups and intraperitoneally injected with either vehicle or 30 mg/kg body weight of ACY-1215 per day, 1 mg/kg body weight of KU-55933 per day, or the same dosages of ACY-1215 plus KU-55933 per day for 5 days per week. The tumor volumes were measured on a weekly basis. The bar graph indicates the averages of tumor volumes ± SEM within each group (n=6-8). ***P<0.001. (E) Following 4 weeks of treatment, the mice were euthanized. The tumors were removed, and images were captured. Representative images of dissected tumors are shown. ****P<0.0001.

the cleaved-PARP was evaluated as the indicator of apoptosis in both MDA-MB-231 and MCF-7 cells. However, MCF-7 is known to have caspase-3 deficiency and relies on caspase-7 alone for PARP degradation (14,15). This is likely the reason why MCF-7 exhibited less prominent PARP degradation than MDA-MB-231 for the double treatment.

Combination of ACY-1215 and KU-55933 or KU-60019 causes markedly stronger inhibition on migration and invasion of MDA-MB-231 cells. It is known that MDA-MB-231 cells have strong migration capability *in vitro* (16). Thus, the effect of combining ACY-1215 with KU-55933 or KU-60019 on migration and invasion of MDA-MB-231 cells was examined. Similar to what it was observed in cell apoptosis and proliferation assays, our results revealed a markedly stronger inhibitory effect on migration (Fig. 4A) and invasion (Fig. 4B and C) of MDA-MB-231 cells when both ACY-1215 and KU-55933 or KU-60019 were used to treat the cells.

Combination of ACY-1215 and KU-55933 causes markedly stronger inhibition on tumor growth than ACY-1215 or KU-55933 alone in mouse tumor xenografts derived from MDA-MB-231 cells. To confirm the *in vitro* results, the effect of combining ACY-1215 and KU-55933 versus ACY-1215 or KU-55933 alone on tumor growth in female nude mice inoculated with MDA-MB-231 cells was further determined. A total of 4 groups of mice with equal tumor burden were treated with the vehicle, ACY-1215, KU-55933, or ACY-1215 plus KU-55933 for four weeks. Treatment with ACY-1215 and/or KU-55933 had no adverse effects on mice, including food intake and body weight. However, mice treated with ACY-1215 and KU-55933 had significantly decreased tumor

size compared with mice treated with only ACY-1215 or KU-55933 (Fig. 4D and E) (17).

Discussion

The crucial role of p53 in preventing tumorigenesis through induction of cell apoptosis, cell cycle arrest(18,19) and maintenance of genomic stability (20-22) render reactivation of mutated p53 one of the most promising therapeutic strategies in cancer therapy. Unfortunately, targeting mutated p53 protein has revealed to be a challenging task, as thus far, there are still no reactivators of p53 mutants available for clinical use (2). However, these failed attempts made it urgent to develop new compounds that could successfully restore function of p53 in TNBC and other subtypes of aggressive cancer.

In the present study, ACY1215 was identified as a novel activator of mutant p53. It was found that ACY1215 causes increased acetylation of p53 not only in MCF-7 (non-TNBC with wild-type p53) but also in MDA-MB-231 cells (TNBC with mutated p53). More importantly, our results revealed that this increased acetylation was accompanied by increased expression of p21, suggesting that ACY1215 may lead to enhanced transcriptional activity of p53. Consistent with these findings, it was demonstrated that ACY1215 treatment resulted in G1 cell cycle arrest and apoptosis in both cell lines.

While ACY-1215 may simply stimulate wild-type p53 transcriptional activity in MCF-7 cells, it may have a distinct and more profound effect on mutant p53 in MDA-MB-231 cells. While mutant p53 lost its transcriptional activity as a monomer, post-translational modifications at its C-terminal, including acetylation at Lys382, may restore mutant p53 to its normal conformation as a tetramer so it could bind to its downstream transcriptional targets, leading to cell cycle arrest and cell apoptosis (1,2). While our results suggested that the increased acetylation of p53 at Lys382 caused by ACY1215 is important for mutant p53 to at least partially recover its wild-type function in MDA-MB-231 cells, the underlying mechanism as to how function of mutant p53 is restored by ACY-1215 requires further investigation.

The reactivation of mutant p53 also poses a great opportunity in combination therapy with other chemotherapeutic compounds to target aggressive subtypes of cancer that are resistant to conventional cancer therapy. As Akt is overactivated in the majority of TNBC and ATM is a stimulator of Akt in cancer cells (9), combination of ACY-1215 with KU-55933/KU-60019 was examined on the proliferation of MDA-MB-231 as well as MCF-7 cells and it was observed that the combination caused a likely additive or synergistic effect on inhibition of proliferation of these cells. Our results further indicated that the suppressive effects on proliferation of these breast cancer cells are likely caused by enhanced cellular apoptosis.

Cells undergoing malignant transformation often exhibit a shift in cellular metabolism from oxidative phosphorylation to aerobic glycolysis (Warburg effect) to survive the tumor microenvironment (23). While p53 and Akt may induce cellular apoptosis through distinct pathways, i.e. p53/PUMA/Noxa or Akt/Bad/Bax, it is also likely they may regulate cell apoptosis through a common pathway. Indeed, it was recently observed that KU-55933 strongly inhibits glucose uptake and glycolysis in aggressive breast and prostate cancer cells, including TNBC cells (12). Our previous results further demonstrated that the ability of KU-55933 to inhibit glucose uptake and glycolysis is closely correlated with its induction of apoptosis (10-12). Interestingly, as a tumor suppressor, p53 is also important in inhibiting glucose uptake and glycolysis by regulating the activities of multiple key enzymes involved in the glucose uptake and glycolysis processes (24,25). It will be interesting to further explore the mechanisms that are responsible for the effects of ACY1215 and KU-55933/KU-60019 on induction of cancer cell apoptosis.

In the present study, it was also demonstrated, for the first time to the best of our knowledge, that combination of ACY1215 and KU-55933 may have an additive or synergistic effect on growth of TNBC-derived breast tumors with no significant side effects. As TNBC represents one of the most malignant subtypes of cancer that are resistant to standard of care cancer chemotherapy, combination of ACY1215 and KU-55933 or their analogs may represent novel chemotherapeutic agents that are highly effective in treating/preventing aggressive cancer and have the potential to replace traditional chemotherapeutic approaches/agents.

In summary, our study has provided novel insights into the molecular mechanisms underlying the function of ACY-1215 in inhibiting cancer cell proliferation and tumor growth and helped to identify ACY-1215 as a novel activator of mutant p53 in cancer cells. Our results have further demonstrated that ACY-1215 may inhibit proliferation of cancer cells through induction of cancer cell cycle arrest and apoptosis. Combination of ACY-1215 and specific ATM inhibitors KU-55933/KU-60019 have also demonstrated their efficacy in inhibiting cancer cell proliferation and motility both *in vitro* and *in vivo* in cell and tumor models of TNBC. Thus, these results may pave the way for future clinical trials testing these compounds in people with high-risk of developing cancer or patients with various types of aggressive cancers for which current chemo- or immunotherapy has limited efficacy.

Acknowledgements

Not applicable.

Funding

The present study was supported by the National Cancer Institute of the National Institutes of Health (grant no. R01CA157012 to MPC), a Grant-In-Aid Award (to DQY) from the University of Minnesota, the Paint-The-Town-Pink Research Grant (to SAG) and the Hormel Foundation.

Availability of data and materials

All data generated or analyzed during this study are included in this published article, and please contact the corresponding authors for any materials described in this study.

Authors' contributions

WC, RS, SR and MJ performed the research. WC, RS and DQY analyzed the data. SAG, DQY, ABDA, MPC, and YL,

supervised the study. RS and DQY wrote the manuscript. YL, MPC, ABDA and SAG critically read and reviewed the manuscript. SAG, DQY and MPC provided funding. DQY and RS confirmed the authenticity of all the raw data. All authors read and approved the final version of the manuscript.

Ethics approval and consent to participate

All the procedures followed in mice experiments were approved by the University of Minnesota IACUC (Minneapolis, MN, USA).

Patient consent for publication

Not applicable.

Competing interests

The authors declare that they have no competing interests.

References

1. Halaby MJ and Yang DQ: p53 translational control: A new facet of p53 regulation and its implication for tumorigenesis and cancer therapeutics. Gene 395: 1-7, 2007.
2. Ji B, Harris BR, Liu Y, Deng Y, Gradilone SA, Cleary MP, Liu J and Yang DQ: Targeting IRES-Mediated p53 Synthesis for Cancer Diagnosis and Therapeutics. Int J Mol Sci 18: 93, 2017.
3. Network TCGA; Cancer Genome Atlas Network: Comprehensive molecular portraits of human breast tumours. Nature 490: 61-70, 2012.
4. Brown CJ, Cheok CF, Verma CS and Lane DP: Reactivation of p53: From peptides to small molecules. Trends Pharmacol Sci 32: 53-62, 2011.
5. Muller PA and Vousden KH: Mutant p53 in cancer: New functions and therapeutic opportunities. Cancer Cell 25: 304-317, 2014.
6. Ryu HW, Shin DH, Lee DH, Choi J, Han G, Lee KY and Kwon SH: HDAC6 deacetylates p53 at lysines 381/382 and differentially coordinates p53-induced apoptosis. Cancer Lett 391: 162-171, 2017.
7. Seidel C, Schnekenburger M, Dicato M and Diederich M: Histone deacetylase 6 in health and disease. Epigenomics 7: 103-118, 2015.
8. Lorenzo Pisarello M, Masyuk TV, Gradilone SA, Masyuk AI, Ding JF, Lee PY and LaRusso NF: Combination of a Histone Deacetylase 6 Inhibitor and a Somatostatin Receptor Agonist Synergistically Reduces Hepatorenal Cystogenesis in an Animal Model of Polycystic Liver Disease. Am J Pathol 188: 981-994, 2018.
9. Li Y and Yang DQ: The ATM inhibitor KU-55933 suppresses cell proliferation and induces apoptosis by blocking Akt in cancer cells with overactivated Akt. Mol Cancer Ther 9: 113-125, 2010.
10. Halaby MJ, Hibma JC, He J and Yang DQ: ATM protein kinase mediates full activation of Akt and regulates glucose transporter 4 translocation by insulin in muscle cells. Cell Signal 20: 1555-1563, 2008.
11. Halaby MJ, Kastein BK and Yang DQ: Chloroquine stimulates glucose uptake and glycogen synthase in muscle cells through activation of Akt. Biochem Biophys Res Commun 435: 708-713, 2013.
12. Harris BRE, Zhang Y, Tao J, Shen R, Zhao X, Cleary MP, Wang T and Yang DQ: ATM inhibitor KU-55933 induces apoptosis and inhibits motility by blocking GLUT1-mediated glucose uptake in aggressive cancer cells with sustained activation of Akt. FASEB J 35: e21264, 2021.
13. Golding SE, Rosenberg E, Valerie N, Hussaini I, Frigerio M, Cockcroft XF, Chong WY, Hummersone M, Rigoreau L, Menear KA, *et al*: Improved ATM kinase inhibitor KU-60019 radiosensitizes glioma cells, compromises insulin, AKT and ERK prosurvival signaling, and inhibits migration and invasion. Mol Cancer Ther 8: 2894-2902, 2009.
14. Jänicke RU, Sprengart ML, Wati MR and Porter AG: Caspase-3 is required for DNA fragmentation and morphological changes associated with apoptosis. J Biol Chem 273: 9357-9360, 1998.
15. Yang XH, Sladek TL, Liu X, Butler BR, Froelich CJ and Thor AD: Reconstitution of caspase 3 sensitizes MCF-7 breast cancer cells to doxorubicin- and etoposide-induced apoptosis. Cancer Res 61: 348-354, 2001.
16. Zhang B, Shetti D, Fan C and Wei K: miR-29b-3p promotes progression of MDA-MB-231 triple-negative breast cancer cells through downregulating TRAF3. Biol Res 52: 38, 2019.
17. Iorns E, Drews-Elger K, Ward TM, Dean S, Clarke J, Berry D, El Ashry D and Lippman M: A new mouse model for the study of human breast cancer metastasis. PLoS One 7: e47995, 2012.
18. Halaby MJ, Harris BR, Miskimins WK, Cleary MP and Yang DQ: Deregulation of Internal Ribosome Entry Site-Mediated p53 Translation in Cancer Cells with Defective p53 Response to DNA Damage. Mol Cell Biol 35: 4006-4017, 2015.
19. Harris BRE, Wang D, Zhang Y, Ferrari M, Okon A, Cleary MP, Wagner CR and Yang DQ: Induction of the p53 Tumor Suppressor in Cancer Cells through Inhibition of Cap-Dependent Translation. Mol Cell Biol 38: 38, 2018.
20. D'Assoro AB, Barrett SL, Folk C, Negron VC, Boeneman K, Busby R, Whitehead C, Stivala F, Lingle WL and Salisbury JL: Amplified centrosomes in breast cancer: A potential indicator of tumor aggressiveness. Breast Cancer Res Treat 75: 25-34, 2002.
21. D'Assoro AB, Busby R, Suino K, Delva E, Almodovar-Mercado GJ, Johnson H, Folk C, Farrugia DJ, Vasile V, Stivala F, *et al*: Genotoxic stress leads to centrosome amplification in breast cancer cell lines that have an inactive G1/S cell cycle checkpoint. Oncogene 23: 4068-4075, 2004.
22. D'Assoro AB, Busby R, Acu ID, Quatraro C, Reinholz MM, Farrugia DJ, Schroeder MA, Allen C, Stivala F, Galanis E, *et al*: Impaired p53 function leads to centrosome amplification, acquired ERalpha phenotypic heterogeneity and distant metastases in breast cancer MCF-7 xenografts. Oncogene 27: 3901-3911, 2008.
23. DeBerardinis RJ, Lum JJ, Hatzivassiliou G and Thompson CB: The biology of cancer: Metabolic reprogramming fuels cell growth and proliferation. Cell Metab 7: 11-20, 2008.
24. Chen JQ and Russo J: Dysregulation of glucose transport, glycolysis, TCA cycle and glutaminolysis by oncogenes and tumor suppressors in cancer cells. Biochim Biophys Acta 1826: 370-384, 2012.
25. Barron CC, Bilan PJ, Tsakiridis T and Tsiani E: Facilitative glucose transporters: Implications for cancer detection, prognosis and treatment. Metabolism 65: 124-139, 2016.